Chemistry & Biology, Vol. 10, 261–270, March, 2003, ©2003 Elsevier Science Ltd. All rights reserved. DOI 10.1016/S1074-5521(03)00050-4

Interaction between Vitamin D Receptor and Vitamin D Ligands: Two-Dimensional Alanine Scanning Mutational Analysis

Mihwa Choi,[1] Keiko Yamamoto,[1,*] Toshimasa Itoh,[1] Makoto Makishima,[2] David J. Mangelsdorf,[3] Dino Moras,[4] Hector F. DeLuca,[5] and Sachiko Yamada[1,*]

[1]Institute of Biomaterials and Bioengineering
Tokyo Medical and Dental University
2-3-10, Kanda-Surugadai
Chiyoda-ku, Tokyo 101-0062
Japan

[2]Department of Organismal Biosystems
Graduate School of Frontier Biosciences
Osaka University
2-2 Yamadaoka
Suita, Osaka 565-0871
Japan

[3]Howard Hughes Medical Institute
Department of Pharmacology
University of Texas Southwestern Medical Center
Dallas, Texas 75390

[4]Laboratoire de Biologie et Genomique Structurale
IGBMC, CNRS
67404 Illkirch
France

[5]Department of Biochemistry
University of Wisconsin
Madison, Wisconsin 53706

Summary

We present a new method to investigate the details of interaction between vitamin D nuclear receptor (VDR) and various ligands, namely a two-dimensional alanine scanning mutational analysis. In this method, the transactivation of various ligands is studied in conjunction with a series of alanine scanning mutations of the residues lining the ligand binding pocket (LBP) of VDR, and the complete set of results is profiled in a patch table. We investigated examples from four structurally diverse groups of known VDR ligands: the native vitamin D hormone and two compounds with the same side chain configuration; four 20-epi compounds; three 19-nor compounds; and two nonsecosteroids. The patch table of the results indicates characteristics of each group in terms of its interaction with 18 LBP residues. We demonstrate the validity of this approach by application to docking studies of the two nonsecosteroids.

Introduction

1α,25-dihydroxyvitamin D_3 [1,25-$(OH)_2D_3$ (**1**)] is a multifunctional hormone. Besides its classical role in regulating calcium and phosphorus metabolism, it is involved in such basic functions as regulation of cell proliferation and differentiation and the immune response. Active vitamin D analogs have been used successfully in the treatment of calcium and bone disorders and the skin disorder psoriasis [1]. However, there is still considerable interest in academia and the pharmaceutical industry in finding vitamin D-related drugs that exhibit specific actions applicable to the treatment of immune disorders, malignant tumors, and disorders of bone formation.

The biological actions of 1,25-$(OH)_2D_3$ (**1**) are mediated mostly through the vitamin D receptor (VDR, NR1I1) [2], a member of the nuclear receptor (NR) superfamily [3,4], to which belong receptors for steroid hormones, retinoids, and thyroid hormone, as well as numerous orphan receptors. The NRs function by regulating the transcription of target genes and generally require their cognate ligands to express their function [5]. When bound to the ligand, the NRs change their conformation to the active form, thereby acting as molecular switches of target gene transactivation [5, 6].

The three-dimensional structures and functions of the NRs have been well studied, affording indispensable information for understanding the mechanism of action of NRs as transcription factors. The 3D structure of the ligand binding domain (LBD) of hVDR has been determined by using a genetically engineered deletion mutant, hVDR LBD (Δ165–215), because the VDR LBD has a long flexible loop between helices 1 and 3 that prevents the preparation of stable crystals for X-ray analysis [7]. Although some ambiguities still remain, the structure of VDR LBD (Δ165–215) has enabled us to analyze ligand potency on the basis of the structure of the LBD. We have been studying the structure-function relationship (SFR) of vitamin D ligands and proposed a simple theory, the space group concept, on the basis of systematic conformational analysis of the ligands and their biological activities [8–12]. We are now studying the SFR of vitamin D ligands in connection with their interaction with the VDR. In this paper we suggest a new approach, two-dimensional analysis. We evaluated the transactivation potency of hVDR induced by various vitamin D ligands in conjunction with systematic one-point mutations of the residues forming the ligand binding pocket (LBP), and the activity profile was analyzed by presenting the results in a patch table. This profiling of the ligand-receptor interaction gives us valuable information on the docking mode of the ligands and, in turn, provides insight into modifying the ligand to create vitamin D drugs with selective function.

In this paper, we investigated the interaction between VDR and ligand using 18 one-point mutants of LBP residues and 12 ligands: 1,25-$(OH)_2D_3$ (**1**), 22-oxa-1,25-$(OH)_2D_3$ (OCT, **2**) [13], 2-hydroxypropoxy-1,25-$(OH)_2D_3$ (ED71, **3**) [14], four 20-epivitamin D analogs (**4–7**) [10, 15], 2-methylene-19-nor-20-epi-1,25-$(OH)_2D_3$ (2MD, **9**) [16] and related compounds (**8** and **10**), and two lithocholic acid derivatives (**11** and **12**) [17] (Figure 1). We also used this approach to verify that the 3D structure of the LBP of the wild-type (wt) VDR is quite similar to that of VDR (Δ165–215).

*Correspondence: yamada.mr@tmd.ac.jp (S.Y.), yamamoto.mr@tmd.ac.jp (K.Y.)

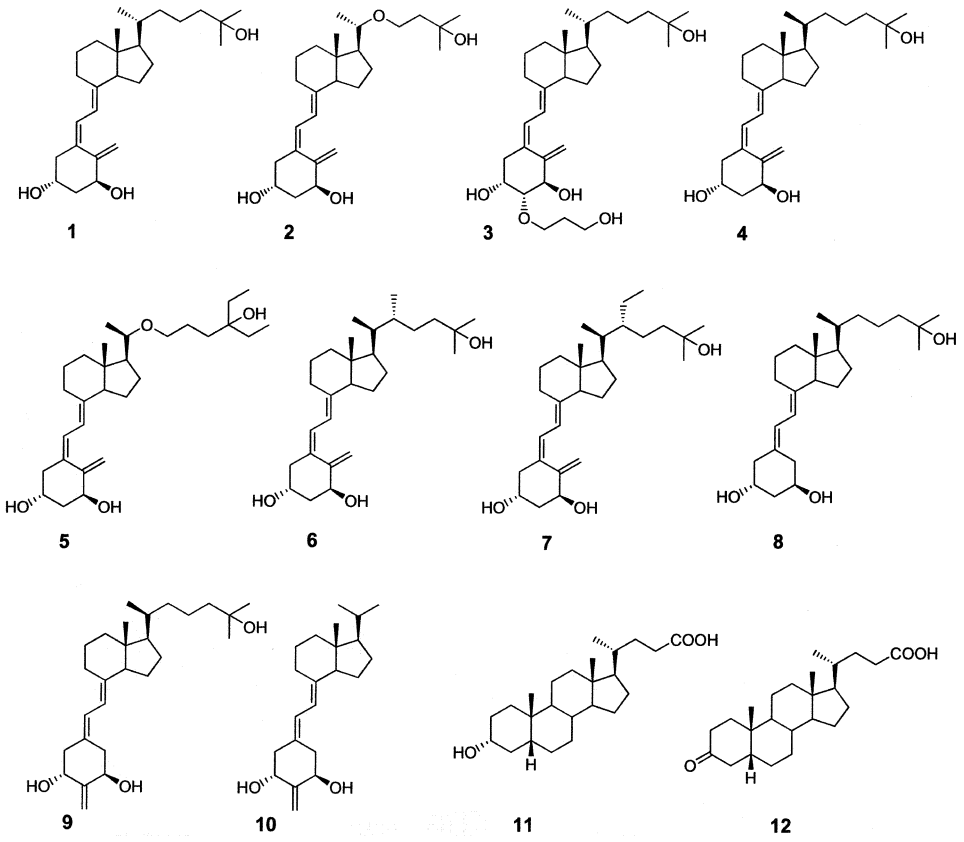

Figure 1. Chemical Structure of VDR Ligands

Results and Discussion

Alanine Scanning Mutagenesis

Alanine scanning mutation has been used frequently to identify functional domains of proteins. We have applied this technique to probe the atomic level interactions between amino acid residues forming the LBP of hVDR and the ligand accommodated in it. We prepared alanine mutants of the residues that were predicted to play key roles (1) in anchoring ligands by hydrogen bonds (Y143, D144, S237, R274, S275, S278, C288, H305, H397, and Q400), (2) in hydrophobic interaction with ligands at the side chain (V234, I268 and V300) and at the seco-B- and C-rings (L233 and W286), and (3) in packing H3 and H4/5 (I271 and V234) and H11 and H12 (Y401), and the residues that change the conformations between the complexes with 20-epi vitamin D analogs and the natural hormone (I238 and I271), viewing the crystal structure of VDR LBD (Δ165–215) [7] (L233A, V234A, S237A, R274A, S275A, S278A, W286A, C288A, H305A, H397A, Q400A, and Y401A were reported in the previous paper [18, 19]). The positions of these mutations are shown in the 3D structure of VDR LBD (Δ165–215) (Figure 2). The expression level and stability of these mutants were evaluated by Western blot analysis and confirmed to be similar to those of the wild-type (Figure 3M) [19]. The transactivation potencies of these mutants with the natural hormone (**1**) and 11 other ligands (**2–12**), including vitamin D analogs and lithocholic acid (LCA) derivatives, were evaluated by dual luciferase assay using a reporter with a mouse osteopontin (OPN) vitamin D response element [20]. The assay results are shown in Figure 3. The roles of individual amino acids, as predicted from the precise 3D structure of hVDR LBD and the current alanine scanning mutational analysis, are summarized in Table 1. Some natural mutants are included for completeness.

Transactivation-Induced by 1,25-$(OH)_2D_3$

Mutation Y143A abolished the transactivation potency of the VDR. Y143, which is located at the corner of H1 to loop 1–3 and interacts with residues at the β-turn (E277), H4/5 (R274), H1 (H139), and loop 1–3 (Y147), probably has a significant role in the folding of the LBD in addition to its role in anchoring the ligand, forming a hydrogen bond with the 3β-hydroxyl group. The 3β-hydroxyl group of 1,25-$(OH)_2D_3$ (**1**) is within a hydrogen bond distance from S278. However, mutation S278A has only a small effect on transactivation [18], indicating the unimportance of this residue either in the interaction with the ligand or in protein folding. Mutation D144A also abolished the transactivation potency of the VDR. D144 might have a major role in the folding of the LBD: its carboxyl group interacts with the main chain NHs of T146 and S148 and its main chain carbonyl interacts with the NH of Y147. It is accepted for many members of the NR family that interaction of H3 and H4/5, either direct or via the ligand, is important for the LBD to maintain its transcriptionally active conformation [21]. In the case of the VDR, I271 (H4/5), I238 (H3), and V234 (H3)

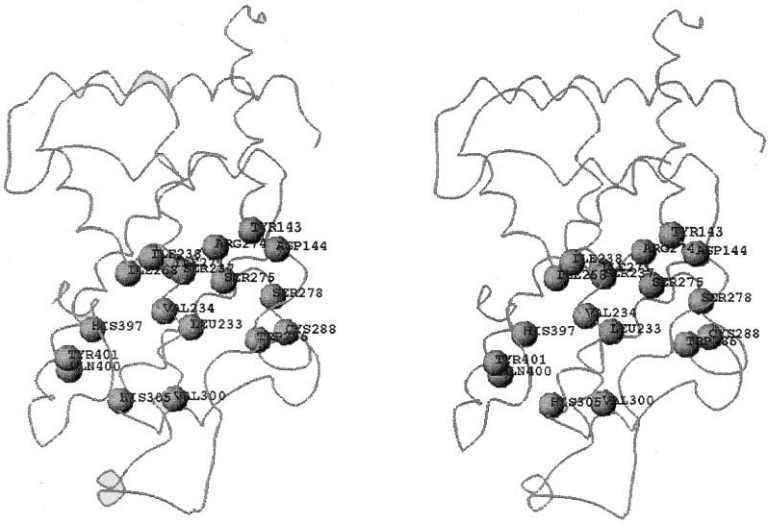

Figure 2. Amino Acid Residues Mutated to Ala in Alanine Scanning Mutation Study

The amino acids mutated to Ala are presented at their Cα positions as gray balls in the VDR-LBD (Δ165–215) (stereoview).

may perform this role: I271 interacts with both I238 and V234. Mutation I271A abolished the transcriptional activity, but the effect of the mutations V234A or I238A was moderate. V234 interacts with the ligand at C(22)H_2 and C(24)H_2, but I238 does not. Interestingly, I271 and I238 change their side chain conformation concomitantly when the 20-epivitamin D analogs, 20-epi-1,25-$(OH)_2D_3$ (MC1288, **4**) and 20-epi-22-oxa-24,26,27-trihomo-1,25-$(OH)_2D_3$ (KH1060, **5**), are accommodated in the LBP, as shown by the X-ray structures of VDR LBD (Δ165–215) complexed with 20-epi-1,25-$(OH)_2D_3$ (**4**) or KH1060 (**5**) [22]. I268 has hydrophobic contacts with C(22)H_2 and C(16)H_2 of 1,25-$(OH)_2D_3$ (**1**) in a triangular relationship and interacts with the residues of H12 (F422) and H11 (H397). Mutation I268A moderately reduced the transactivation potency. The two γ methyl groups of V300 interact with C(21)H_3 and C(12)H_2 of 1,25-$(OH)_2D_3$ (**1**), but mutation V300A has only a moderate effect on the transactivation potency. Mutants not discussed here have been described in our previous paper [19] and their functions are summarized in Table 1.

Transactivation Induced by Other Ligands

We evaluated similarly the transcriptional activities of 11 VDR ligands. The concentration of the ligand was changed depending on the activity of each ligand: 20-epi-1,25-$(OH)_2D_3$ (**4**), KH1060 (**5**), 22-Me-20-epi-1,25-$(OH)_2D_3$ (**6**), 22-Et-20-epi-1,25-$(OH)_2D_3$ (**7**), 19-nor-20-epi-1,25-$(OH)_2D_3$ (**8**), and 2MD (**9**) were assayed at 10^{-10} M; OCT (**2**) and 1α-hydroxy-2-methylene-19-nor-homopregnacalciferol (1-OH-2M-19-nor-homopregnacalciferol, **10**) at 10^{-8} M; ED71 (**3**) at 10^{-7} M; and the least active LCA (**11**) and 3-keto-LCA (**12**) at 10^{-4} M and 3×10^{-5} M, respectively.

The activity spectra of the compounds with a 9,10-secosteroid structure are similar to each other, indicating that these compounds are accommodated in the VDR with a similar docking mode. In fact, the docking mode and hydrogen bonding pattern of 1,25-$(OH)_2D_3$ (**1**), 20-epi-1,25-$(OH)_2D_3$ (**4**), and KH1060 (**5**) in the VDR LBD (Δ165–215) are nearly identical except for their side chain and D-ring regions, as shown by the X-ray structures of the complexes of these ligands with VDR LBD (Δ165–215) [7, 22]. However, each group of compounds has its own characteristics. These characteristics are evident when all the results are displayed in one table.

Two-Dimensional Analysis of the Complete Set of Assay Results

To compare the activity spectra of all the ligands and to identify the characteristics of each compound, we presented the complete set of results in a patch table (Figure 4). In this table, the columns and rows show mutants and ligands, respectively. Ligands are placed in groups according to their structural similarity, and the mutants are ordered so that the more important residues are placed at the top and the less important residues are at the bottom in terms of the activity induced by the natural hormone (**1**). The effects of mutations are categorized into four groups for simplicity and are shown as patches: abolished or significantly reduced activity (<20% of the original activity of wtVDR), solid patch; moderately reduced (20%–60%), gray; slightly affected (61%–90%), dotted; and similar or elevated (>91%), unshaded. Inspection of this table leads to the following conclusions.

First, the upper eight residues (Y143, D144, L233, I271, R274, W286, H397, and Y401) that are essential for the transactivation of VDR induced by 1,25-$(OH)_2D_3$ (**1**) are also essential for vitamin D ligands with full-length carbon chains and the 1α-, 25-, and 3β-hydroxyl groups (**1–9**). Exceptions are 1-OH-2M-19-nor-homopregnacalciferol (**10**) and LCA (**11**). 1-OH-2M-19-nor-homopregnacalciferol (**10**), which has neither the 25-hydroxyl group nor its equivalent, needs no hydrogen bond partner in the LBP facing the side chain terminal. Therefore, mutation H397A did not show a significant effect on transactivation. Mutation L233A showed only a moderate effect on the transactivation induced by LCA (**11**), which has a 5β-cholane structure. L233 plays a key role in binding the ligand by forming van der Waals contacts with the s-*cis* diene part of vitamin D. Therefore, it is reasonable

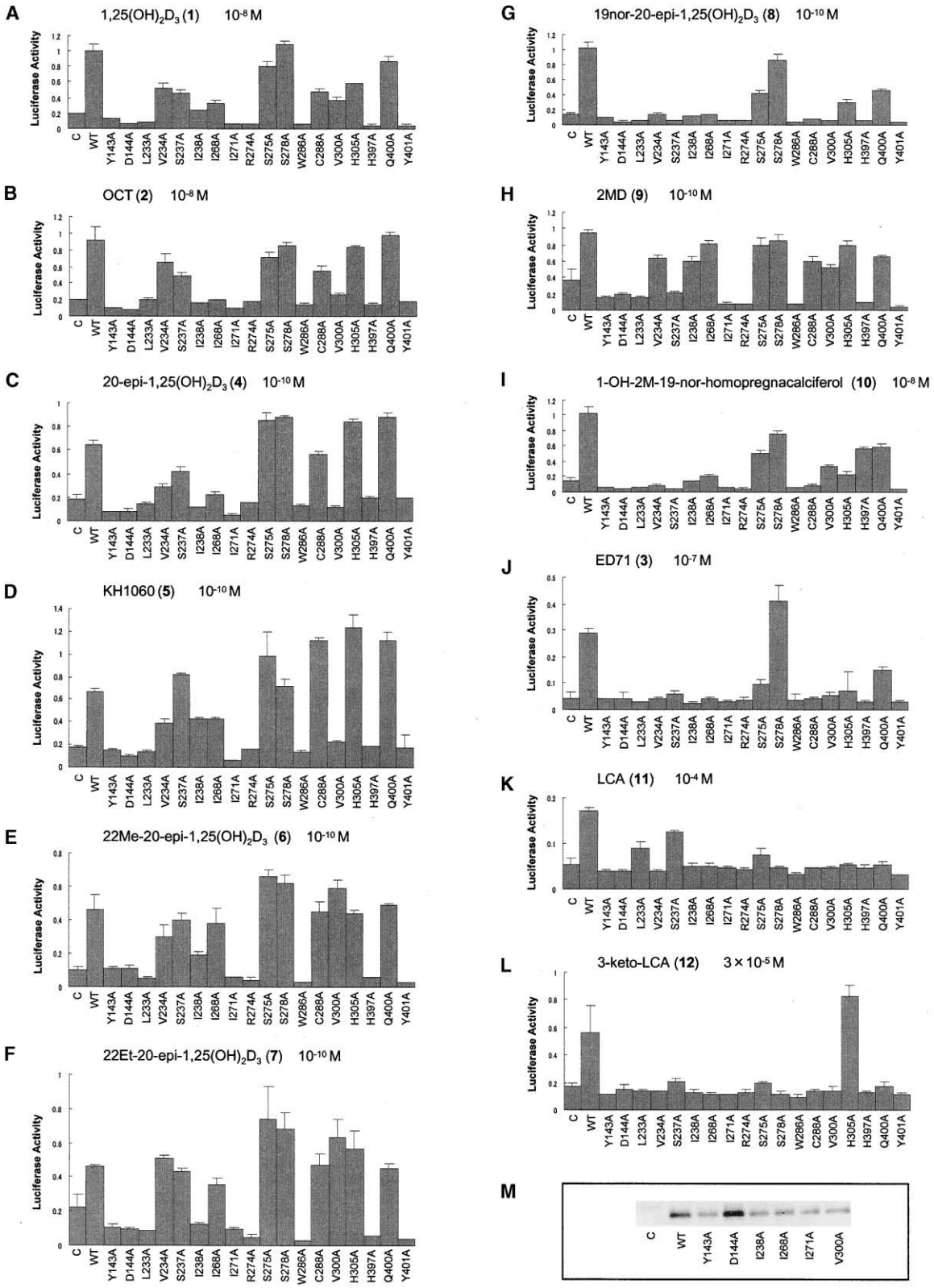

Figure 3. Transcriptional Activities of Wild-Type and 18 One-Point Mutant VDRs Induced by 12 VDR Ligands

(A–L) The results of transactivation assays of 18 mutants stimulated by each of 12 ligands. The activities were evaluated by dual luciferase assay using a full-length hVDR expression plasmid (pCMX-hVDR) and a luciferase reporter gene with a mouse osteopontin VDRE at the promoter (SPPx3-TK-Luc) in COS7 cells.

(M) Immunoblot analysis of wild-type and newly mutated VDRs.

Table 1. Functions of Residues Lining the LBP of hVDR

$1\alpha,25\text{-}(OH)_2D_3$	Amino Acid Residues	Natural Mutant	Location	Assumed Function
A-ring	Y143		H1	Essential for protein folding and/or hydrogen bond with 3β-OH
	D144		Loop 1–3	Essential for protein folding
	S237		H3	Assistant hydrogen bond with 1α-OH
	R274	R274L	H4/5	Hydrogen bond with 1α-OH
	S275		H4/5	Hydrophobic interaction with ligand
	S278		H4/5	Hydrogen bond with 3β-OH
	C288		β sheet	Hydrophobic interaction with ligand
B- and C-rings	L233	L233fs	H3	Hydrophobic interaction with ligand
	W286		β sheet	Hydrophobic interaction with ligand
D-ring and side chain	V234		H3	Hydrophobic interaction with ligand and with H4/5
	I238		H3	Hydrophobic interaction with H4/5
	I268		H4/5	Hydrophobic interaction with ligand
	I271		H4/5	Hydrophobic interaction with ligand and with H3
	V300		H6	Hydrophobic interaction with ligand
	H305	H305Q	Loop 6–7	Assistant hydrogen bond with 25-OH
	H397		H11	Hydrogen bond with 25-OH
	Y401		H11	Hydrophobic interaction with H12

that L233 is not essential for the function of non-9,10-secosteroid ligand LCA (**11**).

Second, for the transactivation by less bulky ligands, importance of bulky hydrophobic residues increases. For example, the mutations I238A and I268A significantly reduced the activity induced by OCT (**2**), which has a less bulky oxygen at the 22-position. For 19-nor-20-epivitamin D (**8**), which lacks the exocyclic methylene group that forms key van der Waals contact with L233, an additional six residues are essential. Introduction of an exocyclic methylene group to the 2-position of 19-norvitamin D **8** (to give 2MD **9** [23]) enormously elevates the activity and at the same time reduces the number of essential residues to nine. This effect is explained by recovered hydrophobic interactions at the 2-methylene group as shown in the docking model of **9** (Figure 5A).

Third, the number of essential residues increases with a decrease in potency of the ligand. For example, the A-ring-modified compound ED71 (**3**) requires additional six residues. The reason may be that in this compound compatibility between the receptor and ligand is partially destroyed.

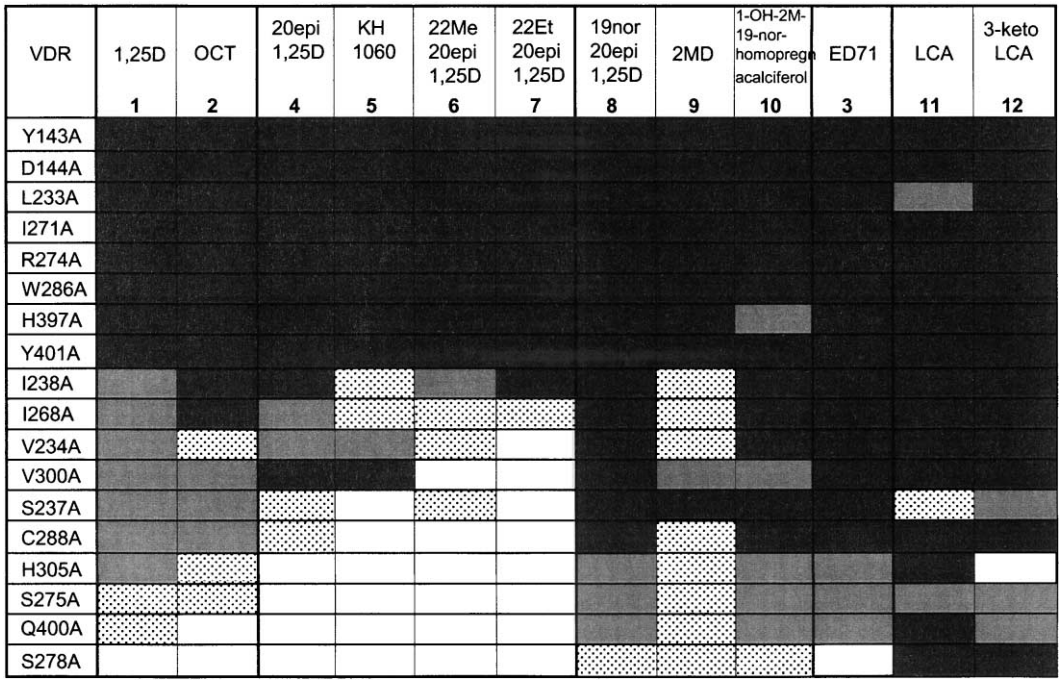

Figure 4. Patch Table Presentation of Transactivation Profiles

Whole sets of transcriptional assay results shown in Figure 3 (A–L) are presented in a patch table where the effects of mutations are categorized in four groups and presented by four kinds of patches: abolished or significantly reduced (<20% of the original activity of wtVDR), solid patch; moderately reduced (20%–60%), gray; slightly affected (61%–90%), dotted; and similar or elevated, unshaded. The columns and rows show mutants and ligands, respectively.

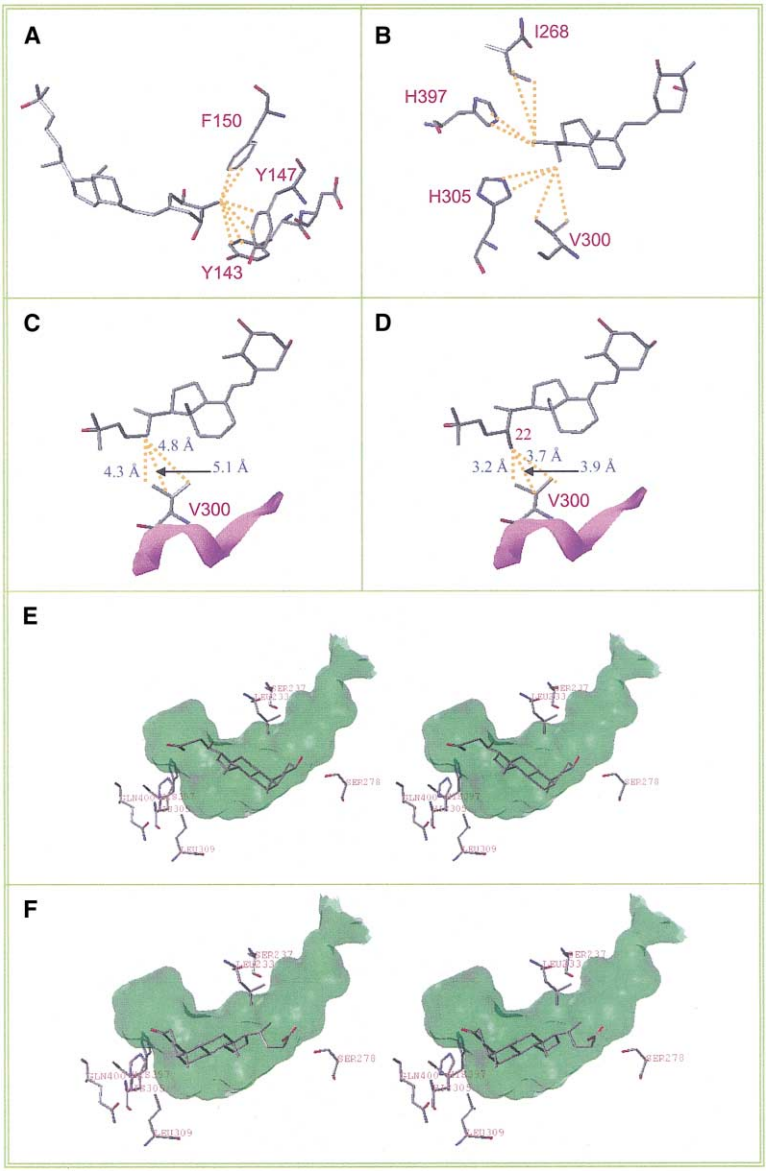

Figure 5. Docking Models of VDR Ligands

Vitamin D ligands, 2MD (**9**) (A), 1-OH-2M-19-nor-homopregnacalciferol (**10**) (B), and 22-Me-20-epi-1,25-$(OH)_2D_3$ (**6**) (D), were docked into VDR LBD (Δ165–215) (PDB: 1IE9) manually. LCA (**11**) (E) and 3-keto-LCA (**12**) (F) were docked into VDR LBD (Δ165–215) (PDB: 1DB1) using the docking software FlexX.

(A) Docking model of 2MD **9** showing putative key hydrophobic interaction of the 2-CH_2 group with hydrophobic amino acid residues.

(B) Symmetrical van der Waals contacts between 1-OH-2M-19-nor-homopregnacalciferol (**10**) and LBP residues that are assumed to be responsible for the high potency of this compound.

(C and D) The interactions of the C(22)H_2 of 20-epi-1,25-$(OH)_2D_3$ (**4**) (C, 1IE9) and the 22-methyl group of **6** (D) with V300 are compared.

(E) LCA (**11**) docked in the VDR LBP and its interacting amino acid residues. The side chain carboxyl group and the 3α-hydroxyl group are within a hydrogen bond distance from H305 and H397 and S278, respectively.

(F) 3-Keto-LCA (**12**) docked in the VDR LBP. The side chain carboxyl group is directed to the β-turn site interacting with S278. The Connolly channel surface of the VDR LBP is shown in translucent green (E and F).

Fourth, for highly active 20-epi analogs (**4–7**), some of the mutations to less bulky residues increase potency, as indicated by increased unshaded patches. These results suggest that highly active compounds have many van der Waals contacts with the VDR, but conversely that these compounds may experience some steric congestion within the LBP.

The activity pattern is characteristic for each type of compound and affords valuable information about ligand receptor interaction and, in turn, about docking mode. As described above, I238 and I268 are essential for the 22-oxa derivative (OCT), suggesting that the hydrophobic interaction with I268 is more important in compound with O(22) than in those with C(22)H_2. V300 is important for two 20-epivitamin D analogs (**4** and **5**), because mutation to Ala abolished transactivation. But this is not true for the 22-alkylated derivatives (**6** and **7**), for which mutation V300A has little effect on potency. We explain these results as follows. V300 forms important van der Waals contact with the 20-epivitamin D analogs **4** and **5** at C(22)H_2 (Figure 5C). Mutation to less bulky Ala eliminates this important interaction in **4** and **5** but not in the 22-alkyl derivatives **6** and **7**, because the alkyl group at C(22) can still have intense interaction with V300A. The docking model of **6** (Figure 5D) shows the effect of 22-alkylation on the interaction with V300. These results clearly explain the reason why 22-alkylation has a high potentiation effect. S237 is important for the group of 19-norvitamin D analogs. Perhaps, to compensate the loss of the van der Waals contact at C(19)H_2 with L233, the importance of the hydrogen bond between S237 and the 1α-hydroxy group increases. It is interesting that 1-OH-2M-19-nor-homopregnacalciferol (**10**) still has transactivation potency similar to that of the natural hormone. In a docking model of **10** (Figure 5B), the short side chain is held very tightly by four van der Waals contacts at the two symmetrical methyl groups: the pro-R methyl group contacts H397 and I268,

and the pro-S methyl group contacts V300 and H305. In addition to the effect of 2-methylene, this may be the reason for the unusual potency of the pentanor compound **10**.

A striking difference in the activity pattern was found for the LCA derivatives, new VDR ligands discovered recently [17]. LCA (**11**) is a secondary metabolite of bile acid produced by microorganisms present in the intestine and is thought to be involved in the development of colon cancer [24]. Since both LCA (**11**) and 3-keto-LCA (**12**) are nearly 10,000-fold less active than 1,25-$(OH)_2D_3$ (**1**) in transactivation, it is reasonable that most residues are essential for transactivation. S278, which is not important for any of the vitamin D ligands tested, is essential for both LCA derivatives **11** and **12**. Interestingly, LCA (**11**) and 3-keto-LCA (**12**) show different patterns in the transactivation. A remarkable difference between **11** and **12** is found in the mutations S237A and H305A (Figures 3K and 3L). The transactivation potency of LCA (**11**) was little affected by the mutation S237A but was abolished by H305A. On the other hand, 3-keto-LCA (**12**) showed the opposite pattern with these mutants. Additional differences are that L233 is important for 3-keto-LCA (**12**) but not so important for LCA (**11**) and that Q400 is important for **11** but not very important for **12**. These differences indicate that the two compounds are docked in the LBP with different modes.

We examined the docking of **11** and **12** in VDR LBD (Δ165–215) by using the docking software FlexX [25, 26] (Tripos, St. Louis). In this analysis, two docking models were suggested for LCA (**11**), one with the side chain directed to H12 (mode 1, Figure 5E) and the other with the side chain harbored deep in the β-turn site (mode 2). Interestingly, only one docking mode was suggested for 3-keto-LCA (**12**), with the side chain directed to the β-turn site (mode 2, Figure 5F). Considering the marked difference found in the transactivation studies, we assume that LCA (**11**) is docked in the LBP with mode 1 (Figure 5E), whereas 3-keto LCA (**12**) is accommodated with mode 2 (Figure 5F). The docking models coincide well with the 2D analysis, as described below.

VDR LBD (Δ165–215)/LCA (Model 1, Figure 5E)

Mutation S237A has little effect on the potency of LCA (**11**), since S237 is distant from ligand **11** in LCA model 1. L233 is also situated a little distance from the ligand, so its mutation to Ala has only a moderate effect. Q400 at H11 does not have direct contact with VDR ligands, but interacts intimately with L309 (H7) as well as H305 (loop 6–7), which, in turn, contacts the ligand. Thus, Q400 is important in stabilizing the architecture of the VDR LBD. The role of Q400 is not evident when the LBP residues have intense contact with the docked ligand, as is the case for vitamin D ligands. For the VDR/LCA complex, where only limited interaction is expected between the LBP and the ligand, the importance of Q400 would be expected to increase.

VDR LBD (Δ165–215)/3-keto-LCA (Figure 5F)

L233 is important for 3-keto-LCA (**12**), because it is assumed to have intimate interaction with the ligand side chain. Mutation of H305 to less bulky Ala has little effect on the activity of 3-keto-LCA (**12**), probably because elimination of a hydrogen bond between H305 and the 3-keto group is compensated by the removal of steric repulsion between the His and the A-ring. For both LCA compounds **11** and **12**, S278 is important, because both ligands are anchored by hydrogen bonds with this residue.

On the Structure of the LBP of Wild-Type hVDR

As described above, Illkirch group has solved the 3D structure of the VDR LBD by using a genetically engineered deletion mutant [7, 22]. Since as many as 51 residues are eliminated from loop 1–3, there remain some ambiguities for the structure of wtVDR LBD. The same authors examined the biological and physicochemical properties of VDR LBD (Δ165–215) to answer the question [27]. They concluded that the eliminated loop is not involved in the main biological function of the VDR, and that loop 1–3 in wtVDR is not well ordered and is highly mobile in solution. In the 2D analysis described above, we found few discrepancies between the transactivation potency displayed by the VDR equipped with a full-length loop 1–3 and the results of docking studies using the crystal structure of VDR LBD (Δ165–215).

Recently, the crystal structures of apo- and holo-PXR LBD have been reported [28]. The PXR is the nuclear receptor structurally most closely related to the VDR, the identity being 44% in the structurally conserved region of the LBDs. Although the PXR LBD contains a long loop between H1 and H3 (Figure 6A), the crystal structures of both the apo- and holo-forms were elucidated including this long loop. The 3D structures of the PXR LBD and VDR LBD (Δ165–215) are very similar, excluding those parts covering H6 to the N terminus of H7. In the PXR LBD, part of the residues of loop 1–3 constitute the bottom of its LBP, but in the crystal structure of VDR LBD (Δ165–215), the residues of H6 to H7 occupy this position. Therefore, if loop 1–3 of the wtVDR has a conformation similar to that of the PXR, H6 of the wtVDR would not form the bottom of the LBP, unlike in VDR LBD (Δ165–215). In that case, the residues V300 (H6) and H305 (H7) would be extruded outside, as for the corresponding residues of the PXR, and would not be able to interact with the ligand (Figure 6B). To answer this question, we made the six mutants Y143A, I238A, S278A, C288A, V300A, and H305A of VDR (Δ165–215) and examined their activity by 2D (3 × 6) analysis with three ligands. As shown in Figures 6D and 6E, the wtVDR and VDR (Δ165–215) showed nearly the same transactivation pattern, indicating that the LBP structures of the two proteins are similar. These results provide additional evidence to support the belief that the 3D structure of the wtVDR LBD is nearly identical to that of VDR LBD (Δ165–215).

Significance

Knowledge of precise ligand-receptor interaction is crucial for determining the exact function of a ligand. In this paper, we developed a new method to investigate the details of a ligand-receptor interaction, namely two-dimensional alanine scanning mutational analysis in which the activity of various vitamin D ligands in a transient transfection assay was studied in

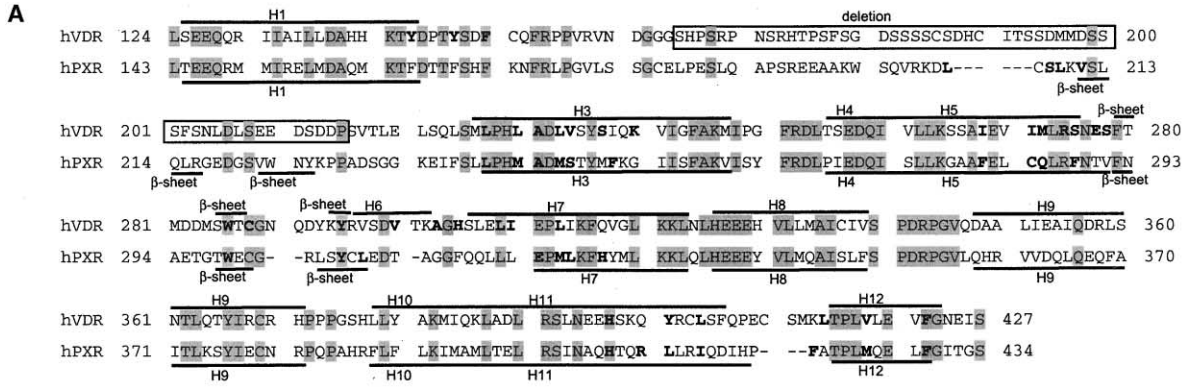
A
deletion
H1
hVDR 124 LSEEQQR IIAILLDAHH KTYDPTYSDF CQFRPPVRVN DGGGSHPSRP NSRHTPSFSG DSSSSCSDHC ITSSDMMDSS 200
hPXR 143 LTEEQRM MIRELMDAQM KTFDTTFSHF KNFRLPGVLS SGCELPESLQ APSREEAAKW SQVRKDL--- ---CSLKVSL 213
β-sheet
H3
H4
H5
β-sheet
hVDR 201 SFSNLDLSEE DSDDPSVTLE LSQLSMLPHL ADLVSYSIQK VIGFAKMIPG FRDLTSEDQI VLLKSSAIEV IMLRSNESFT 280
hPXR 214 QLRGEDGSVW NYKPPADSGG KEIFSLLPHM ADMSTYMFKG IISFAKVISY FRDLPIEDQI SLLKGAAFEL CQLRFNTVFN 293
β-sheet
β-sheet
H6
H7
H8
H9
hVDR 281 MDDMSWTCGN QDYKYRVSDV TKAGHSLELI EPLIKFQVGL KKLNLHEEEH VLLMAICIVS PDRPGVQDAA LIEAIQDRLS 360
hPXR 294 AETGTWECG- -RLSYCLEDT -AGGFQQLLL EPMLKFHYML KKLQLHEEEY VLMQAISLFS PDRPGVLQHR VVDQLQEQFA 370
H10
H11
H12
hVDR 361 NTLQTYIRCR HPPPGSHLLY AKMIQKLADL RSLNEEHSKQ YRCLSFQPEC SMKLTPLVLE VFGNEIS 427
hPXR 371 ITLKSYIECN RPQPAHRFLF LKIMAMLTEL RSINAQHTQR LLRIQDIHP- --FATPLMQE LFGITGS 434

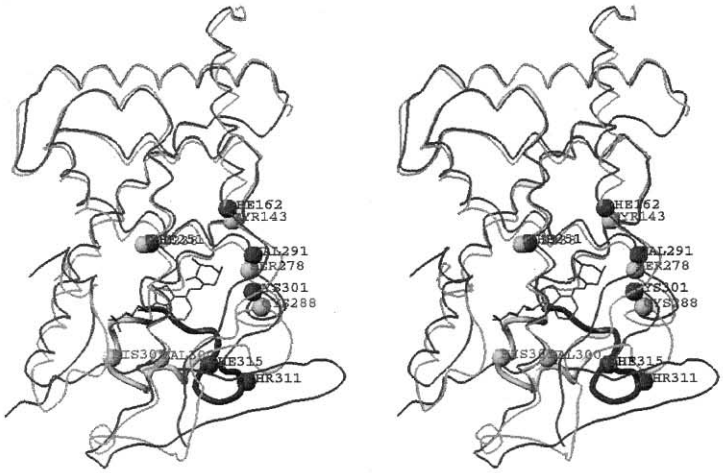
B

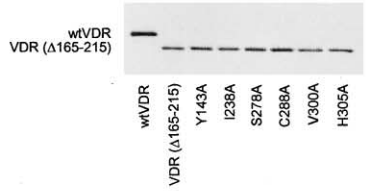
C
wtVDR
VDR (Δ165-215)
wtVDR
VDR (Δ165-215)
Y143A
I238A
S278A
C288A
V300A
H305A

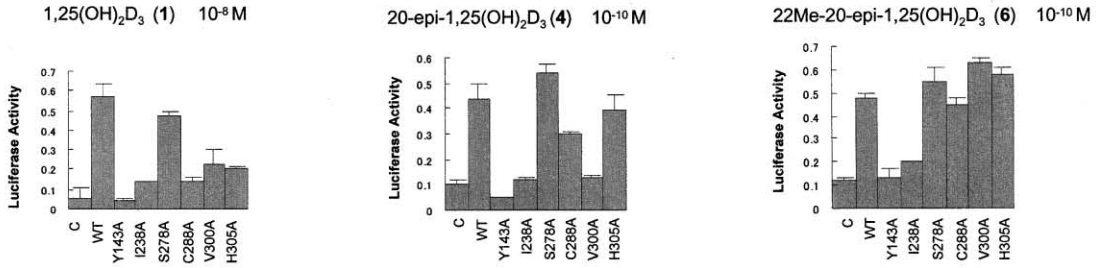
D VDR
1,25(OH)2D3 (1) 10-8 M
20-epi-1,25(OH)2D3 (4) 10-10 M
22Me-20-epi-1,25(OH)2D3 (6) 10-10 M
Luciferase Activity
C
WT
Y143A
I238A
S278A
C288A
V300A
H305A

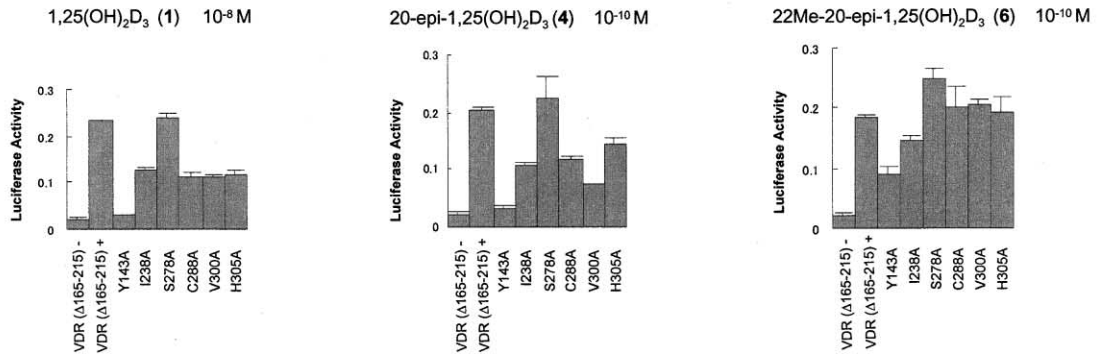
E VDR (Δ165-215)
1,25(OH)2D3 (1) 10-8 M
20-epi-1,25(OH)2D3 (4) 10-10 M
22Me-20-epi-1,25(OH)2D3 (6) 10-10 M
Luciferase Activity
VDR (Δ165-215) -
VDR (Δ165-215) +
Y143A
I238A
S278A
C288A
V300A
H305A

conjunction with a series of alanine scanning mutations of the residues lining the hVDR LBP; the complete set of results was profiled two-dimensionally in a patch table. We investigated examples from four structurally diverse groups of known VDR ligands by this method: the native vitamin D hormone and two compounds with the same side chain configuration; four 20-epi compounds; three 19-nor compounds; and two nonsecosteroids. The 12 × 18 patch table of the results obtained from the assays of 12 ligands with 18 mutants led the following conclusions. (1) The eight residues (Y143, D144, L233, I271, R274, W286, H397, and Y401) are essential for the transactivation by vitamin D ligands. (2) Importance of bulky hydrophobic residues increases for the transactivation by less bulky ligands (8, 10–12). (3) The number of essential residues increases with decreasing potency of the ligand (3, 11, 12). (4) Mutations to less bulky residues tend to increase the potency of highly active 20-epi-ligands (4–7). We demonstrated the validity of this approach by correlation with a docking study of the nonsecosteroidal ligands LCA (11) and 3-keto LCA (12). We are developing this method further to determine the function of H12 in terms of ligand structure, to design new ligands with useful function, and to clarify what factors allow discrimination among the multiple function of this hormone (1).

Experimental Procedures

Compounds

22-Me-20-epi-1,25-$(OH)_2D_3$ (**6**), 22-Et-20-epi-1,25-$(OH)_2D_3$ (**7**) [29], and 19-nor analogs (**8–10**) [30] were synthesized in our laboratory by methods as described [10, 16]. OCT (**2**) and ED71 (**3**) were kindly gifted by Chugai Pharmaceutical Co., Ltd., and MC1288 (**4**) and KH1060 (**5**) were kindly gifted by Leo Company. LCA (**11**) was purchased, and 3-keto-LCA (**12**) was synthesized from **11** in our laboratory.

Site-Directed Mutagenesis

The human VDR (hVDR) expression vectors, pCMX-hVDR [31] and pSG5-hVDR (Δ165–215) [27], were used as a template for in vitro site-directed mutagenesis. Point mutants were created using a QuickChange Site-directed Mutagenesis Kit (Stratagene, CA). Using synthetic oligonucleotides, six clones of mutated hVDRs (Y143A, D144A, I238A, I268A, I271A, and V300A) from pCMX-hVDR and another six clones (Y143A, I238A, S278A, C288A, V300A, and H305A) from pSG5-hVDR (Δ165–215) were produced as described by the manufacturer. *E. coli* DH5α competent cells were transformed with the vectors incorporating the desired mutations. The cDNAs of the clones were purified by Qiafilter Plasmid Maxi-Kit (Qiagen, Valencia, CA), and the presence of the desired mutation was confirmed by DNA sequencing.

Transfection and Transactivation Assay

COS-7 cells were cultured in Dulbecco's modified Eagle's medium (DMEM) supplemented with 5% fetal calf serum (FCS). Cells were seeded on 24-well plates at a density of 2×10^4 per well. After 24 hr, the cells were transfected with a reporter plasmid containing three copies of the mouse osteopontin VDRE (5′-GGTTCAcgaGGT TCA, SPPx3-TK-Luc), a wild-type or mutant hVDR expression plasmid [pCMX-hVDR or pSG5-hVDR (Δ165–215)], and the internal control plasmid containing sea pansy luciferase expression constructs (pRL-CMV) by the lipofection method as described previously [18]. After 4 hr incubation, the medium was replaced with fresh DMEM containing 5% charcoal-treated FCS (HyClone, UT). The next day, the cells were treated with either the ligand or ethanol vehicle and cultured for 24 hr. Cells in each well were harvested with a cell lysis buffer, and the luciferase activity was measured with a luciferase assay kit (Toyo Ink, Inc., Japan). Transactivation measured by the luciferase activity was normalized with the internal control. All experiments were done in triplicate.

Western Immunoblot Analysis

COS-7 cells maintained in DMEM with 5% FCS were seeded in 60 mm dishes at a density of 8×10^5 per dish. After 16 hr, the cells were transfected with a wild-type or mutant hVDR expression plasmid [pCMX-hVDR or pSG5-hVDR (Δ165–215)] by the lipofection method as described above. After 4 hr incubation, the medium was replaced with fresh DMEM containing 1% FCS. Next day the transfected cells were solubilized with Nonidet P-40 (NP-40) lysis buffer (0.5% NP-40, 10 mM Tris-HCl [pH 7.6], 150 mM NaCl, 5 mM EDTA, 2 mM Na_3VO_4, 1 mM phenylmethylsulfonyl fluoride, 5 μg of aprotinin per ml). The lysate was diluted 1.3 times in a sample buffer (4% SDS, 4% β-mercaptoethanol, 125 mM Tris-HCl [pH 6.8], 0.002% BPB, 20% glycerol) and boiled for 2 min. Then 15–20 μg of cellular protein was loaded on 4%–20% Multi SDS-polyacrylamide gels (Daiichi Pure Chemicals, Tokyo). After electrophoretic fractionation, the proteins were electrotransferred to PVDF transfer membranes (Amersham, Hybond-P) using a Transblot apparatus (Bio-Rad) in 25 mM Tris-HCl (pH 7.4), 192 mM glycine, 20% methanol. The membrane was blocked by treating with 5% skim milk (Difco) in TBST buffer (25 mM Tris, 136 mM NaCl, 2 mM KCl, 0.05% Tween 20) for 40 min and was washed three times. The membrane was treated with the primary antibody (9A7γ monoclonal anti-VDR antibody) [32] in TBST buffer for 40 min and washed four times. The membrane was then incubated for 40 min with goat anti-rat IgG HRP-conjugated secondary antibody (Santa Cruz) in TBST buffer and washed four times. hVDR proteins were visualized by chemiluminescence using the Chemiluminescence Reagent (NEN™ Life Science Products, Inc.) according to the manufacturer's instructions.

Graphical Manipulations and Ligand Docking

Graphical manipulations were performed using SYBYL 6.7 (Tripos, St. Louis). The atomic coordinates of the crystal structure of hVDR-LBD (Δ165–215) were retrieved from Protein Data Bank (PDB) (entry 1DB1). Vitamin D analogs were docked into the ligand binding pocket manually, and LCA (**11**) and 3-keto LCA (**12**) were using the docking software FlexX (version 1.11.0). FlexX is a fast-automated docking program that considers ligand conformational flexibility by an incremental fragment placing technique [25, 26]. The active site, which is the term equivalent to the LBP used by the docking software

Figure 6. Comparison of the LBDs of VDR and PXR

(A) Sequence alignment of the LBDs of hVDR and hPXR. Bars above and below the sequences show secondary structures. Identical residues between the two receptors are shaded in light gray. Residues facing the LBP are presented as boldface letters. Deletion part (S165-P215) of the VDR for X-ray analysis is boxed with solid line.

(B) Amino acid residues mutated both in the wtVDR and VDR (Δ165–215). The positions of amino acid residues mutated both in the wtVDR and VDR (Δ165–215) are shown in gray balls at their Cα on the VDR-LBD (Δ165–215) (gray ribbon), and on this structure, PXR LBD (black ribbon) is overlaid together with their amino acid residues (Cα, black balls) at the corresponding sequences to the above VDR residues. Gray and black labels are those of VDR and PXR, respectively.

(C) Immunoblot analysis of wtVDR, VDR (Δ165–215), and the six one-point mutants of the latter VDR (Δ165–215).

(D and E) Transcriptional activities of six one-point mutants of wtVDR as well as of VDR (Δ165–215) induced by three ligands.

FlexX, of the VDR LBD was defined as all amino acids within 6.5 Å proximity of the cocrystallized ligand 1,25-$(OH)_2D_3$ (**1**).

Acknowledgments

We thank Dr. N. Kubodera of Chugai Pharmaceutical Co., Ltd., for the generous gift of OCT and ED71. We thank also Dr. L. Binderup of Leo Company for the generous gift of 20-epi-1,25-$(OH)_2D_3$ and KH1060.

Received: December 2, 2002
Revised: February 11, 2003
Accepted: February 25, 2003

References

1. Kragballe, K. (1997). Psoriasis and other skin diseases. In Vitamin D, D. Feldman, F.H. Glorieux, and J.W. Pike, eds. (San Diego: Academic Press), pp. 1213–1225.
2. DeLuca, H.F. (1990). Mechanism of action of 1,25-dihydroxyvitamin D_3: 1990 version. J. Bone Miner. Metab. *8*, 1–9.
3. Evans, R.M. (1988). The steroid and thyroid hormone receptor superfamily. Science *240*, 889–895.
4. Mangelsdorf, D.J., Thummel, C., Beato, M., Herrlich, P., Schutz, G., Umesono, K., Blumberg, B., Kastner, P., Mark, M., Chambon, P., et al. (1995). The nuclear receptor superfamily: the second decade. Cell *83*, 835–839.
5. Wurtz, J.M., Bourguet, W., Renaud, J.P., Vivat, V., Chambon, P., Moras, D., and Gronemeyer, H. (1996). A canonical structure for the ligand-binding domain of nuclear receptors. Nat. Struct. Biol. *3*, 87–94.
6. Yamada, S., Yamamoto, K., and Masuno, H. (2000). Structure-function analysis of vitamin D and VDR model. Curr. Pharm. Des. *6*, 733–748.
7. Rochel, N., Wurtz, J.M., Mitschler, A., Klaholz, B., and Moras, D. (2000). The crystal structure of the nuclear receptor for vitamin D bound to its natural ligand. Mol. Cell *5*, 173–179.
8. Yamamoto, K., Takahashi, J., Hamano, K., Yamada, S., Yamaguchi, K., and DeLuca, H.F. (1993). Stereoselective syntheses of (22*R*)- and (22*S*)-22-methyl-1α,25-dihydroxyvitamin D_3: active vitamin D_3 analogs with restricted side chain conformation. J. Org. Chem. *58*, 2530–2537.
9. Yamamoto, K., Ohta, M., DeLuca, H.F., and Yamada, S. (1995). On the side chain conformation of 1α,25-dihydroxyvitamin D_3 responsible for binding to the receptor. Bioorg. Med. Chem. Lett. *5*, 979–984.
10. Yamamoto, K., Sun, W.-Y., Ohta, M., Hamada, K., DeLuca, H.F., and Yamada, S. (1996). Conformationally restricted analogs of 1α,25-dihydroxyvitamin D_3 and its 20-epimer: compounds for study of the three-dimensional structure of vitamin D responsible for binding to the receptor. J. Med. Chem. *39*, 2727–2737.
11. Yamada, S., Yamamoto, K., Masuno, H., and Ohta, M. (1998). Conformation-function relationship of vitamin D: conformational analysis predicts potential side chain structure. J. Med. Chem. *41*, 1467–1475.
12. Yamamoto, K., Ooizumi, H., Umesono, K., Verstuyf, A., Bouillon, R., DeLuca, H.F., Shinki, T., Suda, T., and Yamada, S. (1999). Three-dimensional structure-function relationship of vitamin D: side chain location and various activities. Bioorg. Med. Chem. Lett. *9*, 1041–1046.
13. Murayama, E., Miyamoto, K., Kubodera, N., Mori, T., and Matsunaga, I. (1986). Synthetic studies of vitamin D_3 analogues. VIII. Synthesis of 22-oxavitamin D_3 analogues. Chem. Pharm. Bull. (Tokyo) *34*, 4410–4413.
14. Kobayashi, T., Okano, T., Tsugawa, N., Murano, M., Masuda, S., Takeuchi, A., Sato, K., and Nishii, Y. (1993). 2β-(3-hydroxypropoxy)-1α,25-dihydroxyvitamin D_3 (ED-71), preventive and therapeutic effects on bone mineral loss in ovariectomized rats. Bioorg. Med. Chem. Lett. *3*, 1815–1819.
15. Binderup, L., Latini, S., Binderup, E., Bretting, C., Calverley, M., and Hansen, K. (1991). 20-Epi-vitamin D_3 analogues: a novel class of potent regulators of cell growth and immune responses. Biochem. Pharmacol. *42*, 1569–1575.
16. Sicinski, R.R., Prahl, J.M., Smith, C.M., and DeLuca, H.F. (1998). New 1α,25-dihydroxy-19-norvitamin D_3 compounds of high biological activity: synthesis and biological evaluation of 2-hydroxymethyl, 2-methyl, and 2-methylene analogues. J. Med. Chem. *41*, 4662–4674.
17. Makishima, M., Lu, T.T., Xie, W., Whitfield, G.K., Domoto, H., Evans, R.M., Haussler, M.R., and Mangelsdorf, D.J. (2002). Vitamin D receptor as an intestinal bile acid sensor. Science *296*, 1313–1316.
18. Yamamoto, K., Masuno, H., Choi, M., Nakashima, K., Taga, T., Ooizumi, H., Umesono, K., Sicinska, W., VanHooke, J., DeLuca, H.F., et al. (2000). Three-dimensional modeling of and ligand docking to vitamin D receptor ligand-binding domain. Proc. Natl. Acad. Sci. USA *97*, 1467–1472.
19. Choi, M., Yamamoto, K., Masuno, H., Nakashima, K., Taga, T., and Yamada, S. (2001). Ligand recognition by the vitamin D receptor. Bioorg. Med. Chem. *9*, 1721–1730.
20. Noda, M., Vogel, R.L., Craig, A.M., Prahl, J., DeLuca, H.F., and Denhardt, D.T. (1990). Identification of a DNA sequence responsible for binding of the 1,25-dihydroxyvitamin D_3 receptor and 1,25-dihydroxyvitamin D_3 enhancement of mouse secreted phosphoprotein 1 (SPP-1 or osteopontin) gene expression. Proc. Natl. Acad. Sci. USA *87*, 9995–9999.
21. Geller, D.S., Farhi, A., Pinkerton, N., Fradley, M., Moritz, M., Spitzer, A., Meinke, G., Tsai, F.T.F., Sigler, P.B., and Lifton, R.P. (2000). Activating mineralocorticoid receptor mutation in hypertension exacerbated by pregnancy. Science *289*, 119–123.
22. Tocchini-Valentini, G., Rochel, N., Wurtz, J.M., Mitschler, A., and Moras, D. (2001). Crystal structures of the vitamin D receptor complexed to superagonist 20-epi ligands. Proc. Natl. Acad. Sci. USA *98*, 5491–5496.
23. Shevde, N.K., Plum, L.A., Clagett-Dame, M., Yamamoto, H., Pike, J.W., and DeLuca, H.F. (2002). A potent analog of 1α,25-dihydroxyvitamin D_3 selectively induces bone formation. Proc. Natl. Acad. Sci. USA *99*, 13487–13491.
24. Narisawa, T., Magadia, N.E., Weisburger, J.H., and Wynder, E.L. (1974). Promoting effect of bile acids on colon carcinogenesis after intrarectal instillation of N-methyl-N′-nitro-N-nitrosoguanidine in rats. J. Natl. Cancer Inst. *53*, 1093–1097.
25. Rarey, M., Kramer, B., Lengauer, T., and Klebe, G. (1996). A fast flexible docking method using an incremental construction algorithm. J. Mol. Biol. *261*, 470–489.
26. Kramer, B., Rarey, M., and Lengauer, T. (1999). Evaluation of the FLEXX incremental construction algorithm for protein-ligand docking. Proteins *37*, 228–241.
27. Rochel, N., Tocchini-Valentini, G., Egea, P.F., Juntunen, K., Garnier, J.-M., Vihko, P., and Moras, D. (2001). Functional and structural characterization of the insertion region in the ligand binding domain of the vitamin D nuclear receptor. Eur. J. Biochem. *268*, 971–979.
28. Watkins, R.E., Wisely, G.B., Moore, L.B., Collins, J.L., Lambert, M.H., Williams, S.P., Willson, T.M., Kliewer, S.A., and Redinbo, M.R. (2001). The human nuclear xenobiotic receptor PXR: structural determinants of directed promiscuity. Science *292*, 2329–2333.
29. Yamada, S., and Yamamoto, K. September 1998. WO9839292.
30. Sicinski, R.R., Glagett-Dame, M., Plum, L., Deluca, H.F., and Gowlugari, S. August 2002. U.S. patent 6440953.
31. Umesono, K., Murakami, K.K., Thompson, C.C., and Evans, R.M. (1991). Direct repeats as selective response elements for the thyroid hormone, retinoic acid, and vitamin D_3 receptors. Cell *65*, 1255–1266.
32. Pike, J.W., Marion, S.L., Donaldson, C.A., and Haussler, M.R. (1983). Serum and monoclonal antibodies against the chick intestinal receptor for 1,25-dihydroxyvitamin D_3. Generation by a preparation enriched in a 64,000-dalton protein. J. Biol. Chem. *258*, 1289–1296.